The Crystallographic Structure of the B800-820 LH3 Light-Harvesting Complex from the Purple Bacteria *Rhodopseudomonas Acidophila* Strain 7050†

K. McLuskey,‡ S. M. Prince,‡ R. J. Cogdell,§ and N. W. Isaacs*,‡

Department of Chemistry, Division of Biochemistry and Molecular Biology IBLS, University of Glasgow, Glasgow, Scotland G12 8QQ, U.K.

Received February 13, 2001; Revised Manuscript Received May 23, 2001

ABSTRACT: The B800-820, or LH3, complex is a spectroscopic variant of the B800-850 LH2 peripheral light-harvesting complex. LH3 is synthesized by some species and strains of purple bacteria when growing under what are generally classed as "stressed" conditions, such as low intensity illumination and/or low temperature (<30 °C). The apoproteins in these complexes modify the absorption properties of the chromophores to ensure that the photosynthetic process is highly efficient. The crystal structure of the B800-820 light-harvesting complex, an integral membrane pigment−protein complex, from the purple bacteria *Rhodopseudomonas (Rps.) acidophila* strain 7050 has been determined to a resolution of 3.0 Å by molecular replacement. The overall structure of the LH3 complex is analogous to that of the LH2 complex from *Rps. acidophila* strain 10050. LH3 has a nonameric quaternary structure where two concentric cylinders of α-helices enclose the pigment molecules bacteriochlorophyll *a* and carotenoid. The observed spectroscopic differences between LH2 and LH3 can be attributed to differences in the primary structure of the apoproteins. There are changes in hydrogen bonding patterns between the coupled Bchl*a* molecules and the protein that have an effect on the conformation of the C3-acetyl groups of the B820 molecules. The structure of LH3 shows the important role that the protein plays in modulating the characteristics of the light-harvesting system and indicates the mechanisms by which the absorption properties of the complex are altered to produce a more efficient light-harvesting component.

The light-reactions of purple photosynthetic bacteria take place in and on highly invaginated intraplasmic membranes (*1*). The light-energy is initially absorbed by light-harvesting (LH)[1] complexes and then rapidly and efficiently transferred to the reaction centers (RC) (*2*, *3*). The excited RCs use this light-energy to drive a transmembrane charge separation (*4*, *5*). Most purple bacteria produce two types of LH complex (*3*, *6*). The "core" LH1 complex is closely associated with the RC and is present in all species (*6*, *7*). The peripherally arranged LH2 complexes serve to increase the cross-section of the photosynthetic unit and are more abundant when the bacteria are grown at lower light intensities (*8*). Both types of LH complexes are constructed on the same "modular principle". They are oligomers of two low molecular weight, hydrophobic apoproteins (called α and *β*) that noncovalently bind bacteriochlorophyll *a* (Bchl*a*) and carotenoids. Bchl*a* is a porphyrin-like molecule with an asymmetric conjugated double bond system (Figure 1). This *π*-coupled system gives

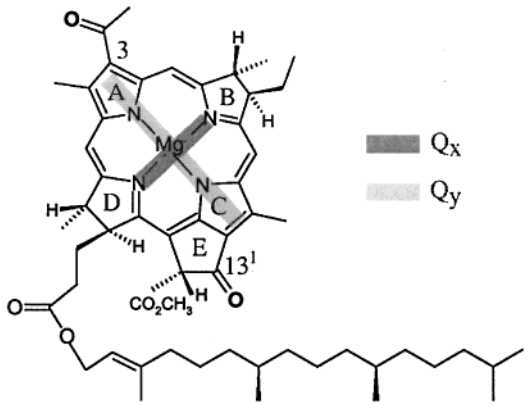

FIGURE 1: Bacteriochlorophyll *a* showing the directions of the Q_x and Q_y dipoles of the bacteriochlorin ring and the numbering of groups referred to in the text.

the molecule two principal absorption characteristics arising from the Q_x and Q_y transition dipoles (*9*). Q_x and Q_y can in turn be mapped to the B,D and A,C ring axes of the bacteriochlorin, respectively (*10*). The Q_y transition dipole, which gives rise to the characteristic absorption of Bchl*a* in LH complexes, has the lower energy (higher wavelength) absorption and is readily influenced by both chromophore coupling and the local environment.

The LH1 complexes have a single, strong, near infrared absorption band between 870 and 890 nm (generalized as absorbing at 875 nm) (Bchl*a*, Q_y band), while the LH2 complexes have two, one at ∼800 nm and the second at ∼850 nm (*3*, *6*, *7*). There is, therefore, an energy gradient

† This work was supported by the Biotechnology and Biological Sciences Research Council and an equipment grant from The Wellcome Trust (Grant 043492).

* To whom correspondence should be addressed. (Tel: +44 (0)141 330 5954; FAX: +44 (0)141 330 4888; E-mail: N.Isaacs@chem.gla.ac.uk).

‡ Department of Chemistry.

§ Division of Biochemistry and Molecular Biology IBLS.

[1] Abbreviations: LH, light-harvesting complex; RC, reaction center; Bchl*a*, bacteriochlorophyll *a*; PC, protomer complex; NCS, noncrystallographic symmetry; *Rps.*, *Rhodopseudomonas*. Atomic coordinates have been deposited with the Protein Data Bank, accession number 1IJD.

10.1021/bi010309a CCC: $20.00
Published on Web 07/06/2001

within the photosynthetic unit from 800 → 850 → 875 nm, and this "funnels" the excitation energy down to the RC (*2*, *7*). Bchl*a* molecules therefore absorb at 800, 850, or 875 nm depending on how they are "packaged" in the protein. This property is one of the key structure/function features of the purple bacterial antenna system, and we would like to understand what factors determine the wavelength where a given Bchl*a* molecule will absorb light.

The structures of a number of peripheral light-harvesting complexes from purple bacteria have been determined. Atomic models of the LH2 complexes from *Rps. acidophila* strain 10050 (*11*) and *Rhodospirillum molischianum* (*12*) are available, along with projection structures of the LH2 complexes from *Rhodovulum sulphidophilum* (*13*) and *Rhodobacter sphaeroides* (*14*). All of these complexes are circular oligomers having a nonameric or octameric quaternary structure.

Some species of purple bacteria, such as *Rps. acidophila* strains 7050 and 7750, when grown at lower light intensities and/or lower temperature turn on the genes that code for a spectral variant of LH2, called LH3 (*9*, *15*, *16*). The near-infrared absorption peaks of LH3 are at approximately 800 and 820 nm (*9*, *15*, *16*). The exact response to these changes in light-intensity varies depending upon the strain of *Rps. acidophila*. Strain 7750 when grown at low light intensity and at 20 °C (the normal growth temperature is 30 °C) almost completely replaces LH2 with LH3 (*16*). In strain 7050, however, LH2 and LH3 always coexist, but the ratio moves strongly in favor of LH3 when the bacteria are grown under low light conditions (*16*). These changes serve to increase the size of the photosynthetic unit and to broaden the spectral range over which solar energy is captured. In the case of strain 7750 grown at low light and low temperature, a reduction of the energy-wasting back transfer from LH1 to LH3 has been established (*17*).

When LH3 complexes were first characterized, it was found that the shift in the Bchl*a* Q_y absorption from 850 to 820 nm was correlated with a change in the primary structure of the apoproteins. A comparison of the amino acid sequences of the apoproteins from *Rps. acidophila* identified certain conserved residues in LH2 complexes that are consistently different in the LH3 complexes (*18*). Within the LH complexes discussed here, this change in the primary structure of the apoproteins is from potential H-bonding residues α44 (Tyr) and α45 (Trp) in LH2 to non-H-bonding α44 (Phe) and α45 (Leu) in LH3.

Resonance Raman spectroscopy indicated that the C3-acetyl oxygens of both the 850 nm absorbing Bchl*a* molecules (B850) were hydrogen-bonded in LH2 (*19*). Fowler et al. (*20*) used site-directed mutagenesis to replace the two putative H-bonding residues from *Rb. sphaeroides* LH2 with two non-H-bonding ones. This genetically modified complex produced a blue-shift in the 850 nm absorption band of the correct magnitude to ~820 nm. From these studies, it was suggested that the loss of these two H-bonds to the C3-acetyl groups of the B850 molecules and the strengthening of another to a B850 $C13^1$-keto group were responsible for the blue-shift in the spectrum. The structure of LH2 from *Rps. acidophila* showed that while αTyr44 and αTrp45 were indeed H-bonded to the acetyl-carbonyls of the two 850 nm absorbing Bchl*a* molecules, there is no H-bonding to keto-carbonyls on any of the B850 molecules (*21*).

Table 1: Data Collection and Structure Determination[a]

Native 1	
spacegroup	*R*32
(hexagonal) unit cell at 100 K	$a = 116.76$, $c = 294.61$ Å
resolution interval	12.5−3.30 Å
R_{merge} multiplicity and completeness	6.9 (12.1)%, 3.3 (2.7), 86.8 (77.4)%
molecular replacement resolution interval	12.0−4.0 Å
solution correlation and R^*_{cryst}	55.2 (39.3)%, 42.4 (48.8)%
Native 2	
(hexagonal) unit cell at 100 K	$a = 117.26$, $c = 295.92$ Å
resolution interval	42.0−3.0 Å
R_{merge} multiplicity and completeness	8.5 (37.0)%, 3.7 (2.9), 97.0 (96.4)%

[a] Items in parentheses denote values for the outer resolution shell, 3.39−3.31 Å, and 3.04−2.95 Å for natives 1 and 2, respectively. Except * where the bracketed terms are the figures for the first incorrect solution.

The position of the Q_y absorption band of Bchl*a* can be influenced by a variety of factors (reviewed in ref *22*). The formation of excitonic coupled aggregates will cause a red-shift of the Q_y absorption relative to that of monomeric Bchl*a* (*23*, *24*). Smaller but significant shifts can also be caused by (i) deformation of the structure of the macrocycle (*25*), (ii) point charges in the local environment of the chromophore (*26*), (iii) rotation of the C3-acetyl group relative to the π-coupled system of the macrocycle (*27*), and (iv) hydrogen-bonding to the C3-acetyl and $C13^1$-keto groups (*28*). We describe below the structure of LH3 and discuss which of these possible factors change when LH3 is compared with LH2.

MATERIALS AND METHODS

The LH3 complex from *Rps. acidophila* strain 7050 was purified and crystallized as described previously (*29*). The critical step in the purification was the separation of the LH3 complex from the LH2 complex by anion-exchange chromatography. Crystals of LH3 were soaked in a mother liquor analogue, and subsequently a cryoprotective solution containing 50% saturated sucrose was introduced in a stepwise manner. X-ray diffraction data were collected, to a resolution of 3.3 Å, on a 30-cm MAR Image plate, with a wavelength of 0.87 Å at station 9.6 of the Daresbury synchrotron. The data set was processed using the program MOSFLM (*30*), and all succeeding computations were performed using programs from the CCP4 suite (*31*). The crystals were found to have the same spacegroup (*R*32) and a similar unit cell to that of the *Rps. acidophila* LH2 complex (*11*).

A comparison of the Patterson functions calculated with the LH2 and LH3 X-ray data showed that the two crystal structures were very similar (the overall correlation coefficient between the two functions was 77%). The 3.3 Å LH3 data set was used to gain a molecular replacement solution using the program AMORE (*32*) (Table 1). The molecular replacement search model was the asymmetric unit of the LH2 complex, comprising one-third of the nonamer with nonidentical residues being trimmed to alanine. An attempt at molecular replacement using the LH2 αβ heterodimer did

Table 2: Refinement[a] of LH3 at 3.0 Å

resolution interval	42.0−3.0 Å
no. parameters	3772
no. reflections ($F > 2\sigma(F)$)	15500
rms deviations from target geometry[b]	0.013, 0.021 Å
R_{cryst}, R_{free} (4.8% reflections)[c,d]	24.3, 25.5%
average B-factor	47.02 Å^2
Sigmaa (*45*) estimated coordinate error	0.39 Å

[a] NCS constrained. [b] Bonded and nonbonded restrained distances. [c] Bulk solvent correction parameters S_{B1} and S_{B2} were refined specifying the correction $f' = f - S_{B1}\exp[-1/2 \cdot S_{B2} \cdot q^2]$ where $q = 2\pi \sin(\theta)/\lambda$. [d] Anisotropic scaling (not applied) over all reflections gives $R_{cryst} = 23.7\%$: $k \exp[b_{11}h^2 + b_{22}k^2 + b_{33}l^2 + 2(b_{12}hk + b_{13}hl + b_{23}kl)]$ where $k = 0.9224$ and $b_{11} = b_{22} = -8.6 \times 10^{-5}$, $b_{33} = -3 \times 10^{-6}$, $b_{12} = -4.3 \times 10^{-5}$, and $b_{13} = b_{23} = 0.0$.

not produce a clear solution. This was thought to be a result of the close association of the protomer complex subunits causing ambiguity in the assignment of inter- and intramolecular vectors. This was also found to be the case in the molecular replacement solution of the LH2 complex from *Rs. Molischianum* where a molecular modeling procedure, to generate the asymmetric unit, was necessary for successful phasing (*12*).

Subsequently, a nearly complete data set was collected under similar conditions at the same synchrotron station. In this case, the cryoprotectant was introduced by dialysis through a 3 kDa membrane, and data were collected to a resolution of 2.8 Å. For the purposes of this study, the resolution was truncated to 3 Å where 50% of the reflections in the outer shell have significance ($I/\sigma(I)$) of better than 2. To eliminate model bias, a coarse omit map was generated by accumulating difference maps and adding the F_o-F_c density arising from the successive omission of 3 Å thick *c*/*z* sections of the search model. The map so produced was back-transformed to give less biased phase estimates. Subsequently three-fold non-crystallographic symmetry (NCS) averaging was performed using a mask defined by the LH2 PC and the C_9 molecular symmetry axis parallel to *c*/*z*.

The indices of the R_{free} (*33*) reflections were the same as those omitted from the *Rps. acidophila* LH2 structural refinement. Model building, using the program O (*34*), primarily consisted of modifying the search model by the replacement of nonequivalent residues and was interspersed with least-squares refinement using the program RESTRAIN (*35*). In all, 60 cycles of refinement were carried out with five stages of model building. NCS was constrained, and a bulk solvent correction was applied throughout the refinement process (Table 2). The LH3 X-ray data were somewhat anisotropic and a $F > 2\sigma(F)$ condition was applied to alleviate this (see Table 2).

Individual isotropic B-factors were refined for all atoms in the LH3 PC and a total of 14 water molecules (one of which is buried close to the B800 site) were added. The water molecules were assigned where density was present in both $2F_o-F_c$ and F_o-F_c maps and where a hydrogen bond to protein could be identified. The protein model comprises residues 1−46 of the α-apoprotein and residues 1−40 of the β-apoprotein. Residues α47−53 and β41−42 could not be assigned from the maps. A Ramachandran plot (*36*) calculated for the protein structure using the program PROCHECK (*37*) shows 94% of residues lie in the most favored regions and the remainder lie in allowed regions. The side chains of residues βGlu7 and βLys7 have very high B-factors, as they are involved in crystal contacts and therefore break the NCS constraint at these contacts. The refined coordinates for the LH3 molecule have been deposited in the Protein Data Bank with the accession code 1IJD.

RESULTS

The overall structure of the LH3 complex is an $\alpha_9\beta_9$ nonamer, similar to the LH2 complex from *Rps. acidophila* (*11*). It is rather like a thick-walled cylinder. The inner walls of the cylinder are formed from nine copies of the transmembrane α-helix of the α-apoprotein and the outer walls from nine copies of the transmembrane α-helix of the β-apoprotein. The pigments (Bchl*a* and carotenoid) are arranged within these two walls of protein, and the whole structure is "capped" top and bottom by the N- and C-termini of both apoproteins folding over and interacting with each other. A detailed description of the LH2 apoprotein structure and its interaction with the pigments has been presented elsewhere (*21*). The Bchl*a* molecules are arranged into two groups. Nine monomeric ones, with their central Mg^{2+} coordinated to an extension of the N-terminal methionine of the α-apoprotein, lie in a ring separated by the outer helices and with the planes of their macrocycles parallel to the plane of the membrane. These Bchl*a* molecules, absorbing at 800 nm, are referred to as B800. Eighteen tightly coupled Bchl*a* (two per αβ-apoprotein pair) have their central Mg^{2+} complexed to conserved histidine residues (α31 and β30) with the planes of their macrocycles perpendicular to the plane of the membrane and parallel to the transmembrane α-helices. These Bchl*a* molecules give rise to the 820 nm absorption band and are therefore referred to as B820 with an α- or β-prefix to indicate the coordinating protein.

In the crystal structure, the asymmetric unit is one-third of the complete nonameric complex. Each asymmetric unit is formed from three protomer complex (PC) subunits, each of which consists of an αβ heterodimer coordinating three Bchl*a* molecules (two contributing to an absorption at 820 nm and the other at 800 nm) and a carotenoid. The nonameric complex is shown schematically in Figure 2 with each asymmetric unit colored differently. An overlay of the LH2 protomer, refined at 2.5 Å resolution, and the LH3 protomer is shown in Figure 3. This comparison was made by superimposing the main chain atoms of LH3 residues α12−36 and β6−37 on the LH2 residues α12−36 and β5−36, respectively. The overall root-mean-square residual for these main chain atoms (comprising the membrane spanning helices) is 0.336 Å after superimposition, suggesting that the LH2 and LH3 subunits are effectively identical at the secondary structure level.

The pigments supported by the protein matrix also overlay well, even though they were not included in the superimposing least-squares target function. The largest deviation between the pigment structures in LH3 and LH2 is a rearrangement in the positioning of the phytyl chain of the αB820 molecule. Within LH2 the phytyl chains and the carotenoid molecule intertwine, suggesting that the mutual interactions between molecules contribute to the overall stability of the complex (*38*). In LH3, the positional shift of the αB820 phytyl chain allows the βB820 phytyl chain, of

FIGURE 2: A schematic diagram of the LH3 nonamer, with the crystallographic asymmetric units in red, green, and blue. The diagram was produced by the program Molscript (*46*).

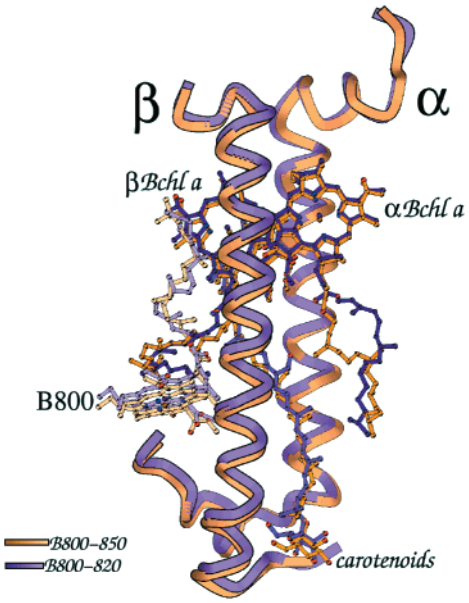

FIGURE 3: A comparison between PCs of LH3 (B800-820, purple) and LH2 (B800-850, tan) (Molscript (*46*) diagram).

an adjacent protomer, to extend further around the pigment array resulting in a slightly tighter chromophore packing arrangement in LH3. Figure 4 illustrates this, showing orthogonal views of the overlaid LH2 and LH3 protomer complexes.

The gross spectroscopic properties of a LH complex are determined by the relative dispositions of the pigments supported by the protein matrix (*39*−*42*). The pigment positions are very similar in both LH2 and LH3 complexes where, in LH3, the coupled Bchl*a* molecules are coordinated by histidine residues at α31 and *β*31 and form a continuous overlapping ring. These B820 molecules lie edge-on to the membrane plane with adjacent pigments having an antiparallel orientation. Overlapping of the bacteriochlorin rings occurs over rings C:C within the individual PC (as shown in Figure 5) and over rings A:A between two adjacent PCs. Consequently, these pigments are in direct contact and produce an exciton coupled band which absorbs at 820 nm.

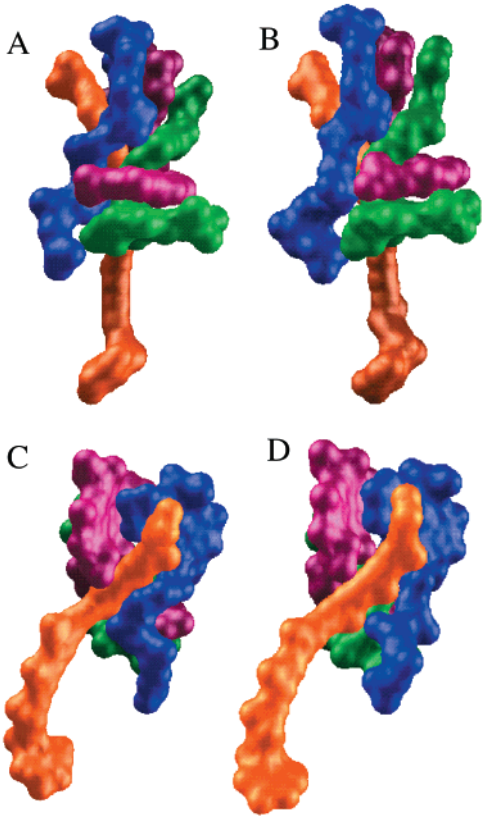

FIGURE 4: Two views of the packing of pigments in LH3 (A and C) and LH2 (B and D). The αB820 and B850 molecules are colored blue, the *β*B820 and B850 molecules are magenta, the B800 molecules are green, and the carotenoid are orange. The major difference between the two complexes is the conformations of the phytyl chains of the αB820 and B850 molecules. These diagrams were produced using the program GRASP (*47*).

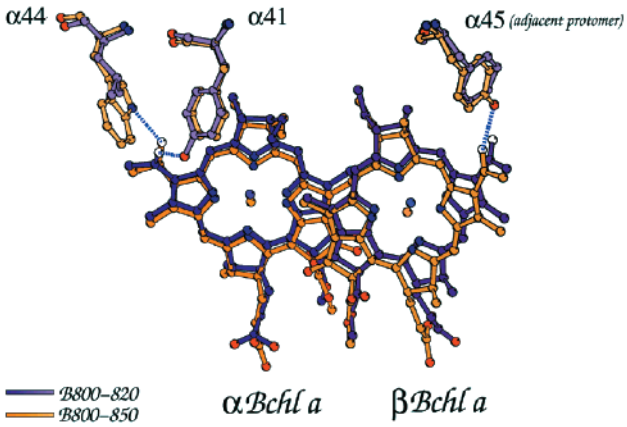

FIGURE 5: Overlays of LH3 B820 (purple) and LH2 B850 (tan) molecules and their H-bond contacts (Molscript (*46*) diagram).

Within the complex, the carotenoid adopts an all trans conformation and is inclined to the membrane normal at an angle of approximately 30°. It is in direct contact with the face of αB820 and also the edge of the B800 Bchl*a* molecules, and there are only van der Waals contacts between the carotenoid and either of the apoproteins. Table 3 summarizes the apoprotein coordination contacts of the three unique Bchl*a* molecules of LH3, the closest pigment−pigment contacts and the Bchl*a* center−center distances. Figure 6 shows omit maps calculated for each of the pigments in LH3, demonstrating the precision with which their relative orientations are known.

Table 3: Contacts to the Pigments of LH3

atom	atom[a]	distance Å
B800 Mg	f-Met α OF	2.49[b]
B800 O3[1]	Arg *β*21 NE	3.08
αB820 Mg	His α31 NE2	2.42[b]
αB820 O3[1]	Tyr α41 OH	2.74
*β*B820 Mg	His *β*31 NE2	2.43[b]
αB820 C2	+*β*B820 C2	3.95
αB820 C12	*β*B820 C12	3.52
carotenoid C26	+αB820 C20	3.93
carotenoid C11	−B800 O13′	3.47
B800 Mg	+αB820 Mg	17.62
B800 Mg	*β*B820 Mg	18.35
αB820 Mg	*β*B820 Mg	9.51
*β*B820 Mg	+αB820 Mg	8.97

[a] ± signs denote adjacent protomers. [b] These contacts were restrained.

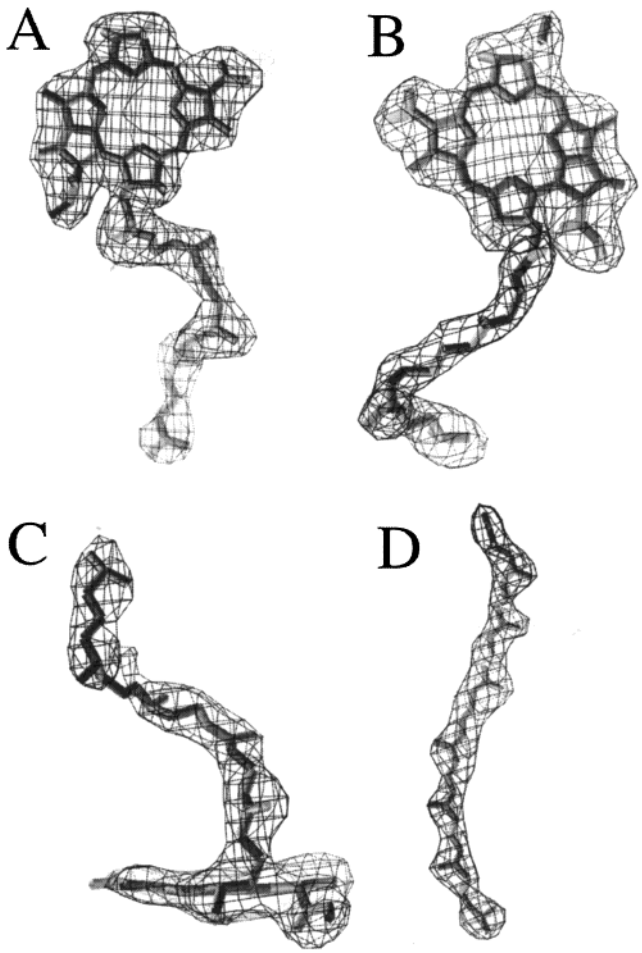

FIGURE 6: F_O-F_C omit maps contoured at 3σ for each of the pigments in LH3 (O (*34*) diagram). (A) αB820, (B) *β*B850, (C) B800, (D) carotenoid.

The major carotenoid reported (*16*) to be present in LH3 was rhodopinal glucoside, a modified form of rhodopin glucoside, the carotenoid found in the LH2 complex. Rhodopinal has a single keto group that replaces a methyl group found in rhodopin (*43*). The expected site of this modification is on the third methyl group (counting from the carotenoid head) of the rhodopin molecule. However, electron density maps for the carotenoid in LH3 show a slightly higher level of density for the fourth methyl group. Since the conjugated double bond system has a symmetrical chemical structure, centered between the third and fourth methyl groups, the two substitutions are chemically equivalent. An oxygen atom was added to the model at each position in turn with appropriate restrained geometry but gave a temperature factor of more than twice the value of the connecting carbon atom. Therefore, our present X-ray model does not provide unambiguous support for the presence of a rhodopinal carotenoid in the LH3 complex. However, it is possible that the rhodopinal carotenoid is present in some of the nine sites in the nonamer, but the limited resolution of this study (3.0 Å), and the imposition of constrained NCS, does not allow us to define this. The glucoside headgroup of the carotenoid is found to be disordered, as is the case in the LH2 structure.

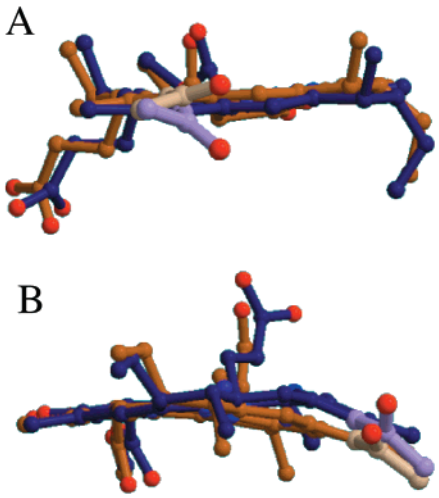

FIGURE 7: Comparison of the conformations of the bacteriochlorin rings in LH3 (purple) and LH2 (tan). (A) αB820/850 molecules, (B) *β*B820/850 molecules. The C3-acetyl groups are colored light purple in the LH3 molecules and cream in the LH2 molecules (Molscript (*46*) diagram).

There are differences between the LH2 and LH3 complexes at the tertiary structural level. As stated previously, a double mutation at positions α44 and α45 is correlated with the spectral shift in the LH3 complex. The structure of LH2 showed that these residues (Trp and Tyr, respectively) made hydrogen bonds to the C3-acetyl groups of the coupled B850 molecules (*11*). The equivalent residues in the LH3 structure are Phe and Leu, which are unable to form hydrogen bonds. The contacts to the bacteriochlorin rings of the B820 molecules in LH3 are listed in Table 3. The *β*B820 molecule is coordinated, through its central Mg^{2+} to a His residue. There are no H-bonds to either the C3-acetyl group or the C13[1]-keto group of the bacteriochlorin. The αB820 molecule is also centrally coordinated to a His residue and again there is no H-bonding to the C13[1]-keto oxygen. However, this molecule does have a hydrogen bond from the C3-acetyl group to αTyr41. This hydrogen bond is not present in the LH2 complex where the residue at the equivalent position is Phe. These changes in the H-bonding patterns between the two complexes are shown in Figure 5.

The consequences of the change in hydrogen bonding patterns between the LH2 and LH3 complexes are rotations of the C3-acetyl groups of both B820 molecules relative to the corresponding positions of these groups on the B850 molecules (Figure 7). The αB820 C3-acetyl group torsion angle (C2−C3−C3[1]−O3[1]) is 132°, and the *β*B820 C3-acetyl torsion angle is 135°. The equivalent B850 values are −166° and 156°, respectively (*21*).

DISCUSSION

Since the structures of the LH3 and the LH2 complexes are very similar (Figures 3, 4, and 5), the difference in the near infrared absorption of these two complexes must therefore arise from either relatively small structural changes of the coupled Bchl*a* or changes within their environments. The chromophoric regions of the pigments in LH3 have essentially the same geometry as those in LH2. The most striking difference is in the arrangement of the phytyl chain of the αB820 molecule. However, as the phytyl chain is fully saturated, this rearrangement cannot explain the changed absorption properties of LH3, and a more detailed comparison of the B820 molecules from LH3 with the B850 molecules from LH2 is therefore necessary.

The location of the generic absorption bands (at 820 nm in LH3 and 850 nm in LH2) is largely the result of excitonic coupling of the Bchl*a* Q_y absorption in the overlapping ring of 18 coupled Bchl*a*'s (*20*, *22*, *27*, *28*, *39*, *40*). In very general terms, when pigments are strongly (Coulombically) coupled this results in the establishment of a manifold of excitonic states. This causes a red-shift of the composite absorption bands, where the exact geometry of the coupled array determines which of the excitonic states have the most oscillator strength. Important factors in determining the energy of the absorption band are the distance between the chromophores and the relative directions of their Q_y transition dipole moments (*23*, *24*, *39*−*42*). The center-to-center separations (measured as $Mg^{2+}-Mg^{2+}$ distances) of the B850 Bchl*a*'s in LH2 are 9.5 and 8.9 Å within and between the PCs (*21*, *38*) and are the same as the $Mg^{2+}-Mg^{2+}$ separations in LH3 (Table 3). As the direction of the Q_y transition dipole of the Bchl*a* molecules is identical in both LH2 and LH3 (*42*), other factors must be responsible for the shift in the position of the Q_y absorption band.

As described in the introduction, there are a number of possible mechanisms by which the "site-energy" of a Bchl*a* molecule can be modulated (*23*−*28*). (i) *Deformation of the structure of the macrocycle:* None of the bacteriochlorin rings of the three different Bchl*a* molecules in LH2 (αB850, βB850 and B800) are completely planar (*21*). The monomeric B800 molecules are slightly domed, the βB850 molecules are bowed around an axis parallel to the line between the bacteriochlorin rings A and E, while the αB850 molecules are nearly planar. Deformation of the bacteriochlorin ring produces red-shifts of the Bchl*a* Q_y absorption band (*25*). However, deformations in LH3 bacteriochlorin structures are not significantly different from those in LH2 (at least at 3 Å resolution). (ii) *Point charges:* Point charges close to the bacteriochlorin ring could produce large shifts in absorption, with the magnitude and direction of the shift depending upon both the size and the sign of the charge and its exact location (*26*). There are no point charges close to the strongly coupled Bchl*a* molecules in either LH2 or LH3. (iii) *Rotation of the C3-acetyl group:* Gudowska-Nowak et al. (*27*) showed how the energy of the Q_y absorption of Bchl*a* could be altered by rotation of the C3-acetyl group relative to the plane of the conjugation in the bacteriochlorin macrocycle. When the acetyl group is in the plane of the bacteriochlorin ring, it adds one more double bond to the conjugated system and the Q_y absorption is red-shifted. As this acetyl rotates out of the plane of conjugation, the Q_y absorption moves toward the blue and as it rotates back into the plane of conjunction the Q_y absorption again shifts toward the red. In the LH2 complex, the deviations of the α- and βB850 acetyl groups from coplanarity with the bacteriochlorin macrocycle are 14 and 24°, respectively. These acetyl groups are rotated further out of the plane in LH3 to 48 and 45° respectively. According to Gudowska-Nowak et al. (*27*), the consequence of this will be to blue-shift the site-energies of both the α- and βB820 molecules in LH3 by an estimated 25 nm relative to the corresponding B850 Bchl*a* molecules in LH2. This could explain most of the blue-shift of the absorption spectrum of the strongly coupled Bchl*a* molecules in LH3 relative to LH2. An effect similar to this was also seen within the "special pair" of Bchl*a* molecules in a site-directed mutant (RM197) of the *Rb. sphaeroides* reaction center (*44*). In this case, the acetyl group is rotated by 20° further out of coplanarity with the bacteriochlorin macrocycle and the absorption maximum of the "special pair" is blue-shifted by 15 nm. (iv) *Hydrogen bonding:* There are no hydrogen bonds made to any of the Bchl*a* $C13^1$-keto groups in either LH2 or LH3. Hydrogen bonds to the C3-acetyl groups will cause a red-shift relative to the non-hydrogen bonded case (*28*), and hence the loss of the hydrogen bond of the C3-acetyl of the β-B850 molecule may also contribute to the overall blue-shift.

In summary, at the present resolution of the LH3 structure, it appears that the major cause of the shift in absorption from 850 nm in LH2 to 820 nm in LH3 is the rather subtle rearrangement of the C3-acetyl groups relative to the plane of the bacteriochlorin macrocycle. As predicted, the blue-shift in the complex can be attributed to a change in the hydrogen bonding patterns between the protein and the pigments. However, the formation of an unexpected H-bond, along with the observed rotations of the acetyl positions, shows that the blue-shift in the absorption spectrum is a consequence of these rearrangements rather than due to a direct result of a loss of H-bonds. Higher resolution data will be required to establish whether any other smaller structural changes also contribute to the total blue-shift.

REFERENCES

1. Clayton, R. K., and Sistrom, W. R. (1978) *The Photosynthetic Bacteria*, Plenum Press, London and New York.
2. van Grondelle, R., Dekker, J. P., Gillbro, T., and Sundstrom, V. (1994) *Biochim. Biophys. Acta 1187*, 1−65.
3. Zuber, H., and Brunisholz, R. A. (1991) in *The Chlorophylls* (Scheer, H., Ed.) pp 627−704, CRC Press, Boca Raton, FL.
4. Deisenhofer, J., Epp, O., Miki, K., Huber, R., and Michel, H. (1985) *Nature 318*, 618−624.
5. Feher, G., Allen, J. P., Okamura, M. Y., and Rees, D. C. (1989) *Nature 339*, 111−116.
6. Zuber, H., and Cogdell, R. J. (1995) in *Anoxygenic Photosynthetic Bacteria* (Blankenship, R. E., Madigan, M. T., and Bauer, C. E., Eds.) pp 315−348, Kluwer Academic Publications, Dordrecht.
7. Cogdell, R. J., Isaacs, N. W., Howard, T. D., McLuskey, K., Fraser, N. J., and Prince, S. M. (1999) *J. Bacteriol. 181*, 3869−3879.
8. Aargaard, J., and Sistrom, W. (1972) *Photochem. Photobiol. 15*, 200−225.
9. Angerhofer, A., Cogdell, R. J., and Hipkins, M. F. (1986) *Biochim. Biophys. Acta 848*, 333−341.
10. Scheer, H. (1991) in *The Chlorophylls* (Scheer, H., Ed.) pp 3−30, CRC Press, Boca Raton, FL.

11. McDermott, G., Prince, S. M., Freer, A. A., Hawthornthwaite-Lawless, A. M., Papiz, M. Z., Cogdell, R. J., and Isaacs, N. W. (1995) *Nature 374*, 517−521.
12. Koepke, J., Hu, X., Muenke, C., Schulten, K., and Michel, H. (1996) *Structure 4*, 581−597.
13. Savage, H., Cyrklaff, M., Montoya, G., Kuhlbrandt, W., and Sinning, I. (1996) *Structure 4*, 243−252.
14. Walz, T., Jamieson, S. J., Bowers, C. M., Bullough, P. A., and Hunter, C. N. (1998) *J. Mol. Biol.* 833−845.
15. Cogdell, R. J., Durant, I., Valentine, J., Lindsay, J. G., and Schmidt, K. (1983) *Biochim. Biophys. Acta 722*, 427−435.
16. Gardiner, A. T., Cogdell, R. J., and Takaichi, S. (1993) *Photosyn. Res. 38*, 159−167.
17. Deinum, G., Otte, S. C. M., Gardiner, A. T., Aartsma, T. J., Cogdell, R. J., and Amesz, J. (1991) *Biochim. Biophys. Acta 1060*, 125−131.
18. Brunisholz, R., and Zuber, H. (1988) in *Photosynthetic Light-Harvesting Systems* (Scheer, H., and Schneider, S., Eds.) pp 103−114, Walter de Gruyter & Co., New York.
19. Fowler, G. J. S., Sockalingum, G. D., Robert, B., and Hunter, C. N. (1994) *Biochem. J. 299*, 695−700.
20. Fowler, G. J. S., Visschers, R. W., Grief, G. G., van Grondelle, R., and Hunter, C. N. (1992) *Nature 355*, 848−850.
21. Prince, S. M., Papiz, M. Z., Freer, A. A., McDermott, G., Hawthornthwaite-Lawless, A. M., Cogdell, R. J., and Isaacs, N. W. (1997) *J. Mol. Biol. 268*, 412−423.
22. Cogdell, R. J., Isaacs, N. W., Freer, A. A., Arrelano, J., Howard, T. D., Papiz, M. Z., Hawthornthwaite-Lawless, A. M., and Prince, S. (1997) *Prog. Biophys., Mol. Biol. 68*, 1−27.
23. Kasha, M., Rawls, H. R., and Ashraf El-Bayoumi, M. (1965) *Pure Appl. Chem. 11*, 371−392.
24. Pearlstein, R. M. (1991) in *The Chlorophylls* (Scheer, H., Ed.) pp 1047−1078, CRC Press, Boca Raton, FL.
25. Barkigia, K. M., and Fajer, J. (1993) in *The Photosynthetic Reaction Center Vol II* (Deisenhofer, J., and Norris, J., Eds.) pp 513−539, Academic Press, San Diego.
26. Eccles, J., and Honig, B. (1983) *Proc. Natl. Acad. Sci. U.S.A. 80*, 4959−4962.
27. Gudowska-Nowak, E., Newton, M. D., and Fajer, J. (1990) *J. Phys. Chem. 94*, 5795−5801.
28. Hanson, L. K., Thompson, M. A., and Fajer, F. (1987) in *Progress in Photosynthesis Research* (Biggins, B. J., Ed.) pp 311−314, Martinus Nihoff, Dordrecht.
29. McLuskey, K., Prince, S. M., Cogdell, R. J., and Isaacs, N. W. (1999) *Acta Crystallogr. D55*, 885−887.
30. Leslie, A. G. W. (1992) in *Joint CCP4 and ESF-EACMB Newsletter on Protein Crystallography, No. 26*, SERC Daresbury Laboratory, Warrington, UK.
31. Collaborative Computational Project Number 4. (1994) *Acta Crystallogr. D50*, 760−763.
32. Navaza, J. (1994) *Acta Crystallogr. A50*, 157−163.
33. Brunger, A. T. (1992) *Nature 355*, 472−475.
34. Jones, T. A., Zou, J. Y., Cowan, S. W., and Kjeldgaard, M. (1991) *Acta Crystallogr. A47*, 110−119.
35. Driessen, H., Haneef, M. I. J., Harris, G. W., Howlin, B., Khan, G., and Moss, D. S. (1989) *J. Appl. Crystallogr. 22*, 510−516.
36. Ramachandran, G. N., and Sasisekharan, V. (1968) *Adv. Prot. Chem. 23*, 284−438.
37. Laskowski, R. A., Macarthur, M. W., Moss, D. S., and Thornton, J. M. (1993) *J. Appl. Crystallogr. 26*, 283−291.
38. Freer, A., Prince, S., Sauer, K., Papiz, M., Hawthornthwaite-Lawless, A., McDermott, G., Cogdell, R., and Isaacs, N. W. (1996) *Structure 4*, 449−462.
39. Sauer, K., Cogdell, R. J., Prince, S. M., Freer, A., Isaacs, N. W., and Scheer, H. (1996) *Photochem. Photobiol. 64*, 564−576.
40. Alden, R. G., Johnson, E., Nagarajan, V., Parson, W. W., Law, C. J., and Cogdell, R. G. (1997) *J. Phys. Chem. B101*, 4667−4680.
41. Hu, X. C., Damjanovic, A., Ritz, T., and Schulten, K. (1998) *Proc. Natl. Acad. Sci. U.S.A. 95*, 5935−5941.
42. Koolhaas, M. H. C., van der Zwan, G., Frese, R. N., and van Grondelle, R. (1997) *J. Phys. Chem. B101*, 7262−7270.
43. Frank, H. A., and Cogdell, R. J. (1993) in *Carotenoids in Photosynthesis* (Young, A., and Britton, G., Eds.) pp 252−326, Chapman & Hall, London.
44. McAuley-Hecht, K. E., Fyfe, P. K., Ridge, J. P., Prince, S. M., Hunter, C. N., Isaacs, N. W., Cogdell, R. J., and Jones, M. R. (1998) *Biochemistry 37*, 4740−4750.
45. Read, R. J. (1986) *Acta Crystallogr. A42*, 140−149.
46. Kraulis, P. J. (1991) *J. Appl. Crystallogr. 24*, 946−950.
47. Nicholls, A., Sharp, K. A., and Honig, B. (1991) *Proteins: Struct., Funct., Genet. 11*, 281−296.

BI010309A